Journal of Power Sources 195 (2010) 5201–5205

Contents lists available at ScienceDirect

Journal of Power Sources

journal homepage: www.elsevier.com/locate/jpowsour

Short communication

Performance of large-scale anode-supported solid oxide fuel cells with impregnated $La_{0.6}Sr_{0.4}Co_{0.2}Fe_{0.8}O_{3-\delta}$+$Y_2O_3$ stabilized ZrO_2 composite cathodes

Jing Chen [a], Fengli Liang [a], Dong Yan [a], Jian Pu [a,*], Bo Chi [a], San Ping Jiang [a,b], Li Jian [a]

[a] School of Materials Science and Engineering, State Key Laboratory of Material Processing and Die & Mould Technology, Huazhong University of Science and Technology, Wuhan, Hubei 430074, China
[b] School of Mechanical and Aerospace Engineering, Nanyang Technological University, Singapore 639798, Singapore

ARTICLE INFO

Article history:
Received 21 January 2010
Received in revised form 20 February 2010
Accepted 22 February 2010
Available online 26 February 2010

Keywords:
Anode-supported solid oxide fuel cells
Nano-structured
Wet impregnation
Cathode
Stability

ABSTRACT

Anode-supported planar solid oxide fuel cells (SOFCs) with an active area of 81 cm^2 (9 cm × 9 cm) and nano-structured $La_{0.6}Sr_{0.4}Co_{0.2}Fe_{0.8}O_{3-\delta}$ + Y_2O_3 stabilized ZrO_2 (LSCF + YSZ) composite cathodes are successfully fabricated by tape casting, screen printing, co-firing and solution impregnation, and tested using H_2 fuel and air oxidant at various flow rates. Maximum power densities of 437 and 473 mW cm^{-2} are achieved at 750 °C by loading 0.6 and 1.3 mg cm^{-2} of LSCF in the composite cathodes, respectively. The gas flow rates, particularly the air, have a significant effect on the cell performance. Cell performance degradation with time is also observed, which is considered to be associated with the growth and coalescence of the nanosized LSCF particles in the composite cathode. The use of the LSCF cathode in combination with YSZ electrolyte without a Gd-doped CeO_2 (GDC) buffer layer is proved to be applicable in large cells, even though the thermal stability of the nanosized LSCF needs to be further improved.

1. Introduction

The reduction of operating temperature of solid oxide fuel cells (SOFCs) from conventional high temperatures near 1000 °C to intermediate temperatures between 600–800 °C is beneficial for increasing the long-term stability of fuel cells and widening the breadth of materials selection, thus reducing the cost of SOFC systems. However, the cell performance is also decreased as a result of reduced operating temperature due to increased resistances in electrodes and electrolyte [1–3]. The electrolyte resistance can be minimized by using thin film electrolyte and/or alternative electrolyte materials with higher ionic conductivity at intermediate temperatures, such as doped lanthanum gallate and ceria [4,5]; however, development of cathodes with low polarization lose and high stability remains challenge for intermediate temperature SOFCs (IT-SOFCs).

Electrochemical performance of an electrode strongly depends on its microstructure; and nano-structured microstructures obtained by wet impregnation technique have been shown to significantly enhance the performance of the electrodes in SOFCs [6,7]. There are two approaches for development of nano-structured electrodes by impregnation techniques. One is to introduce nano-sized catalytically active oxide or metal particles to the conventional electrodes such as Ni/YSZ cermet anodes and Sr-doped $LaMnO_3$ (LSM) cathodes [8–13]; another is to impregnate catalyst nano-particles into the ionic conducting scaffold such as YSZ [14–17].

Mixed ionic and electronic conducting (MIEC) perovskites, such as (La, Sr)(Co, Fe)O_3, have been under intensive investigation as promising cathode materials for intermediate and low temperature SOFCs [18,19]. With much higher oxygen ionic conductivity than that of the conventional cathode material LSM for high temperature SOFCs, (La, Sr)(Co, Fe)O_3-type perovskites have been proved to be highly active for the O_2 reduction reaction in IT-SOFCs [20]. But, this type of materials is likely to chemically react [21] and thermally incompatible [22] with the most reliable Y_2O_3 doped ZrO_2 (YSZ) electrolyte at high temperatures, and their use in combination with YSZ electrolyte is practically limited.

In order to take full advantage of (La, Sr)(Co, Fe)O_3-type perovskites and YSZ electrolyte, efforts have been made to prepare nano-structured electrodes via solution impregnation [6], such as Sr-doped $LaCoO_3$ (LSCo)-YSZ [14] and Sr-doped $LaFeO_3$ (LSF)-YSZ [15]. In a recent study [17], the authors have demonstrated an impregnated composite cathode $La_{0.8}Sr_{0.2}Co_{0.5}Fe_{0.5}O_{3-\delta}$ (LSCF) + YSZ with an electrode polarization resistance as low as 0.047 Ω cm^2 at 750 °C for the O_2 reduction reaction. Nevertheless, the majority of reported results of the nano-structured electrodes made by solution impregnation were obtained from button cells with a small active area; and the effectiveness of such prepared

* Corresponding author at: 1037 Luo Yu Road, Wuhan, Hubei 430074, China. Tel.: +86 27 87558142; fax: +86 27 87558142.
E-mail address: pujian@hust.edu.cn (J. Pu).

0378-7753/$ – see front matter © 2010 Elsevier B.V. All rights reserved.
doi:10.1016/j.jpowsour.2010.02.061

electrodes in large planar cells has not been confirmed so far. The performance of small button cells does not necessarily represent the performance of larger cells as the scalability of electrodes, particularly the cathode, is a major concern in the development of SOFCs [23].

In the present study, we take a different approach from that employed in previous development of impregnated cathodes by using large-scale anode-supported planar SOFC cells (active area 9 cm × 9 cm) as the vehicle to evaluate the effect of the impregnated LSCF + YSZ cathodes on the cell performance at various temperatures with H_2 fuel and air oxidant. The purpose of this study is to demonstrate the possibility of using LSCF cathode material in combination with YSZ electrolyte in large-scale SOFC cells, without the presence of a Gd-doped CeO_2 (GDC) buffer layer in between LSCF and YSZ.

2. Experimental

Fig. 1 shows the procedure for fabricating the planar anode-supported cells with an active area of 9 cm × 9 cm and nano-structured LSCF + YSZ composite cathodes. The anode substrates were produced by tape casting using a slurry containing NiO (Inco. Type A, USA) and YSZ (Tosoh TZ-8YS, Japan) powders at a weight ratio of 40 to 60. The anode functional layer (AFL) of 40 wt.% NiO (Inco. Type F, USA) and 60 wt.% YSZ (Tosoh TZ-8YS, Japan), and YSZ electrolyte (Tosoh TZ-8Y, Japan) were screen printed on the dried tape-cast substrate in sequence. The tape-cast/screen-printed assembly was dried at ambient temperature for 10 h, debindered at a rate of 1 °C min^{-1} and sintered at 1370 °C for 3 h to obtain porous anode and dense electrolyte. To prepare an YSZ porous structure on top of the dense YSZ electrolyte, a layer of YSZ (Tosoh TZ-8YS, Japan) slurry was screen printed, followed by sintering at 1200 °C for 0.5 h in air. The thickness of the porous YSZ layer was ~9 μm. The LSCF impregnation solution was prepared from $La(NO_3)_3{\cdot}6H_2O$, $Sr(NO_3)_2$, $Co(NO_3)_2{\cdot}6H_2O$, $Fe(NO_3)_3{\cdot}9H_2O$ (Sinopharm Chemical Reagent Co. Ltd.) and fluorocarbon surfactant, isopropyl alcohol and deionized water.

The LSCF impregnation solution was prepared from $La(NO_3)_3{\cdot}6H_2O$, $Sr(NO_3)_2$, $Co(NO_3)_2{\cdot}6H_2O$, $Fe(NO_3)_3{\cdot}9H_2O$ (Sinopharm Chemical Reagent Co. Ltd.) and fluorocarbon surfactant, isopropyl alcohol and deionized water. Impregnation was carried out by dropping the LSCF nitrite solution into the pre-sintered porous YSZ scaffold, and then fired at 800 °C in air for 1 h. The formation of perovskite LSCF phase under this condition was confirmed by X-ray diffraction [17]. The loading of LSCF was increased by repeating the impregnation process in order to achieve sufficient conductivity of the nano-structured LSCF + YSZ electrodes. Two similar cells were prepared with different LSCF loadings in the LSCF + YSZ composite cathodes, ~0.6 mg cm^{-2} for Cell-1 and ~1.3 mg cm^{-2} for Cell-2, respectively. The weight fraction of the LSCF in YSZ scaffold was about 17 wt.% for Cell-1 and 37 wt.% for Cell-2. Ni mesh and screen-printed $LaCo_{0.4}Ni_{0.6}O_{3-\delta}$ paste were used as current collectors for the anode and cathode, respectively.

The cell was sealed in the testing jig under compressive load by cast tape seals (alumina), and the NiO-YSZ anode substrate was reduced in situ during start up and at 750 °C for 12 h in flowing N_2–5%H_2 atmosphere before cell testing. The current–voltage data were recorded in the temperature range of 600–750 °C using a SOFC testing system (SF-30, Lixing Testing Equipment, Ltd.) with current density change in between 0 and 1 A cm^{-2}. H_2 and air were flowed to the anode and cathode, respectively, at a rate of 2 L min^{-1}.

In order to identify the mechanism for performance degradation of the cells with impregnated LSCF cathodes, a half-cell, which had a LSCF + YSZ working electrode (LSCF loading ~0.6 mg cm^{-2} and active surface area 0.5 cm^2) and a YSZ electrolyte (1.3 mm thick), was employed as a vehicle to isolate the effect of cathode on cell performance. The cathode performance was measured at a constant current density of 200 mA cm^{-2} against a Pt counter electrode opposite to the cathode and a Pt ring reference electrode located ~5 mm away from the working electrode. Electrochemical impedance spectra were taken in a frequency range of 0.1 Hz to 100 kHz with a signal amplitude of 10 mV at temperatures between 600 and 750 °C using an impedance/gain phase analyzer (Solartron 1260) and an electrochemical interface analyzer (Solartron 1287) at open circuit. A Sirion 200 scanning electron microscope (SEM) was employed to examine the microstructure of the cells before and after the testing.

3. Results and discussion

Fig. 2 shows the performance of the Cell-1 and Cell-2 measured at different temperatures under the flow condition of 4 L min^{-1} H_2 and 4 L min^{-1} air. The open circuit voltage (OCV) is in between 1.182 and 1.220 V for both cells at temperatures between 600 and 750 °C, indicating a robust sealing was achieved for the test of the cells. For the Cell-1 with 0.6 mg cm^{-2} impregnated LSCF in the cathode, the maximum power density decreases from 437 mW cm^{-2} at 750 °C to 210 mW cm^{-2} at 600 °C (Fig. 2a). With the increase of LSCF loading to 1.3 mg cm^{-2}, the maximum power density is increased in the Cell-2 to 473 and 301 mW cm^{-2} at the same temperatures as above. It is understood that the voltage loss at low current density is mainly contributed by activation polarizations of the electrodes. From Fig. 2, it can be seen that at current den-

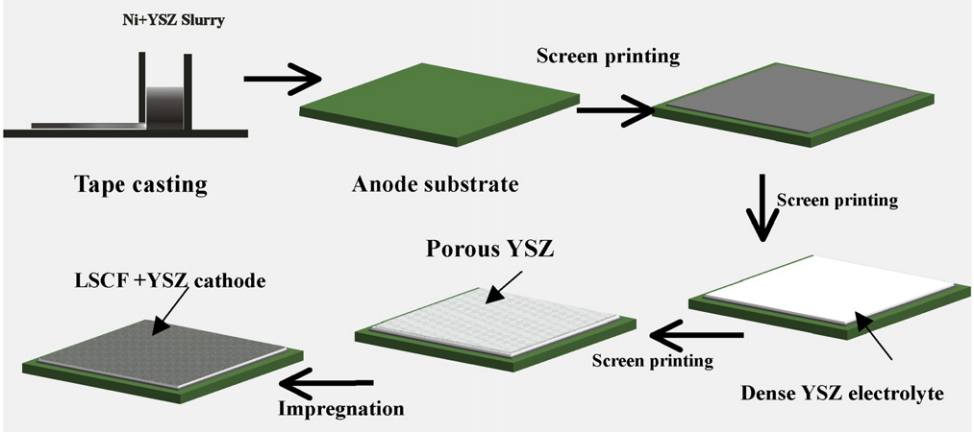

Fig. 1. Procedures to fabricate a planar anode-supported SOFC with nano-structured LSCF + YSZ cathode by impregnation technique.

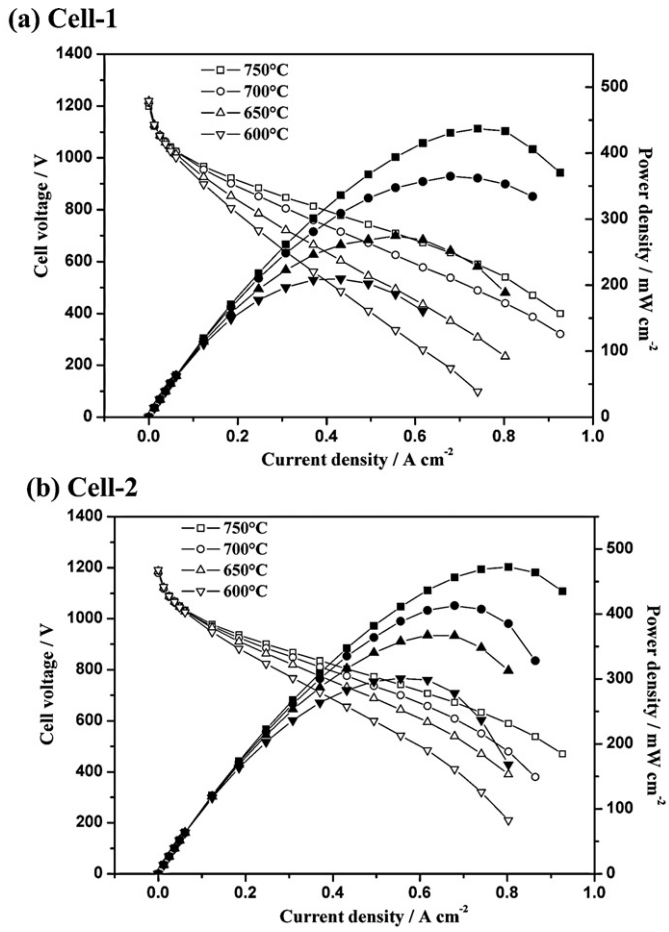

Fig. 2. Cell performance of the anode-supported planar cells with impregnated LSCF + YSZ composite cathode measured at different temperatures under 4 L min^{-1} of H_2 and 4 L min^{-1} of air: (a) Cell-1, LSCF loading ~0.6 mg cm^{-2} and (b) Cell-2, LSCF loading ~1.3 mg cm^{-2}.

sities lower than 0.05 A cm^{-2}, the voltage of both the cells falls from the OCV gradually, with a higher voltage for the Cell-2 than the Cell-1 at 0.05 A cm^{-2}; however, no significant difference can be observed among those obtained at various testing temperatures. This suggests that the impregnated LSCF cathode possesses an excellent electrocatalytic activity at temperatures above 600 °C and increasing LSCF loading improves the electrochemical activity of the cathode. Also seen in Fig. 2, the "ohmic loss" contributed by the electrolyte, electrodes and contact interfaces between electrodes and current collectors is increased as testing temperature is lowered and such loss can be decreased by increasing the amount of the impregnated and electronically conductive LSCF. There is a potential disadvantage associated with the increase of LSCF loading in the cathode, that is, overloading the cathode with the LSCF may result in lack of porosity for gas diffusion in the composite cathode, especially at low testing temperature of 600 °C. Further optimization of LSCF loading is necessary for achieving a higher cell performance.

The effect of air and hydrogen flow rates on cell performance at 750 °C is shown in Fig. 3, with the result obtained from the Cell-2 as an example. It is clearly presented that the change of flow rates does not vary the activation and ohmic losses; nevertheless, the voltage loss associated with gas diffusion is significantly affected. At a constant H_2 flow rate of 2 L min^{-1} on the anode side, the maximum power density of the cell decreases rather significantly from 452 to 373 mW cm^{-2} as the air flow rate changes from 6 to 2 L min^{-1}. On the other hand, at a constant air flow of 4 L min^{-1} on the cathode side, the peak power density decreases from 473 mW cm^{-2} at 4 L min^{-1} of H_2 to 435 mW cm^{-2} at 2 L min^{-1} of H_2. According to the calculation of H_2 and air usage [24], the supply of fuel and oxidant gases was excessive at the peak power density for all the cases, which indicates that the reduction of peak power density with decreasing gas flow rate is not caused by the shortage of gas supply; and the critical issue is the access of fuel and oxidant gases to the reaction sites of the electrodes. It is also can be seen from Fig. 3 that the air flow rate affects the cell performance more significantly than the H_2 flow rate in this specific test, and therefore the concentration polarization caused by the impregnated composite cathode seems to be more decisive on the cell performance. Fig. 4 is the SEM micrograph of the post-test LSCF + YSZ cathode in Cell-2. It clear shows, on one hand, that the impregnated LSCF particles are well connected to ensure adequate electrical conductivity of the cathode; and on the other hand, the surface of the impregnated cathode appears to be densely packed with nanosized LSCF particles, which are considered to obstruct air flow into the cathode and result in considerable dependence of cell performance on air flow rate.

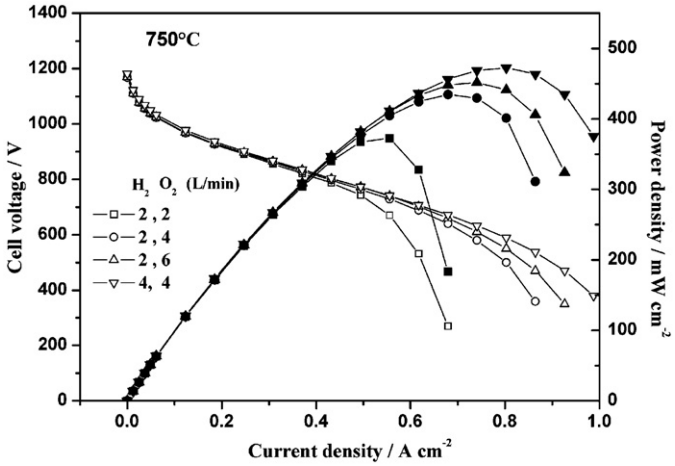

Fig. 3. Performance of Cell-2 under various flow rates of air on the cathode side and H_2 on the anode side.

The performance stability of the Cell-1 was studied at 750 °C, in comparison to that of a small half-cell with 0.6 mg cm^{-2} of LSCF

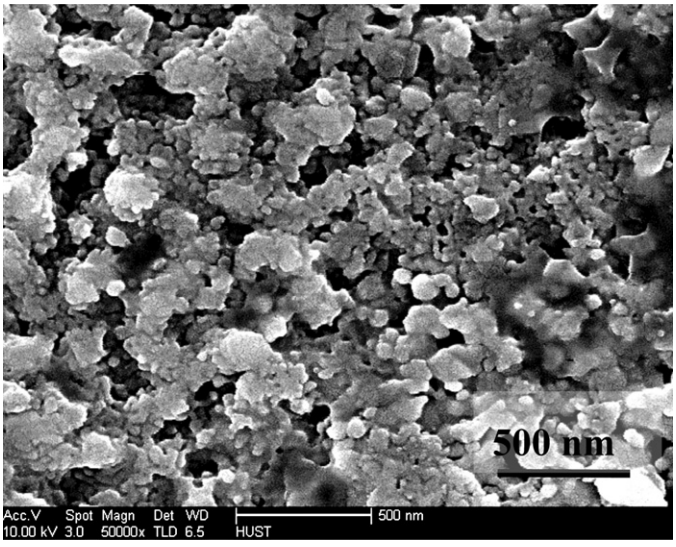

Fig. 4. SEM micrograph of post-test LSCF + YSZ cathode in Cell-2, showing a densely packed morphology of impregnated LSCF particles in porous YSZ structure.

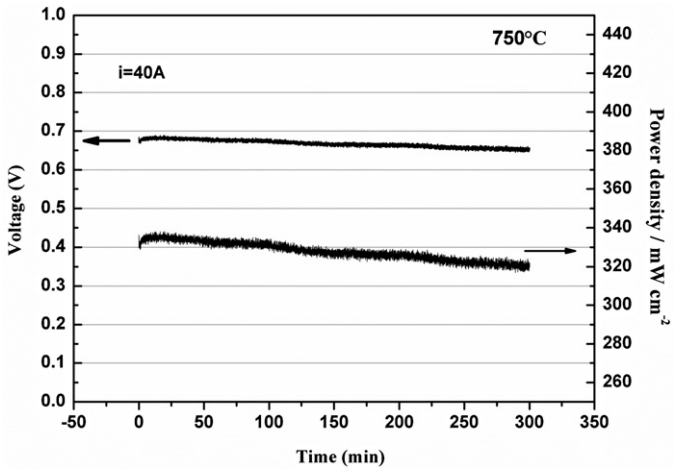

Fig. 5. Performance stability of Cell-1 at 750 °C, with LSCF + YSZ composite cathode. The current density for Cell-1 is 494 mA cm^{-2}.

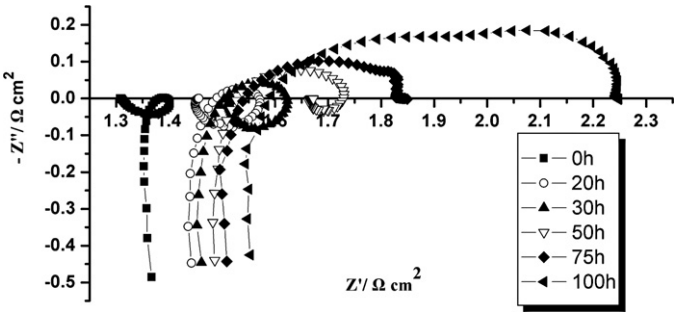

Fig. 6. Impedance spectra of the button half-cell as a function of cathodic current passage of 200 mA cm^{-2} for 100 h.

impregnated in the composite cathode; the results are shown in Fig. 5. In the case of the Cell-1, a current of 40 A was applied over an effective area of 81 cm^2 (~500 mA cm^{-2}) during the durability test. The voltage decreases from 0.684 to 0.650 V in 5 h, showing a significant high degradation of ~5%. In the case of the half-cell, both the polarization and ohmic reissitances of the cathode at 750 °C in air increased with the time of cathodic current passage at 200 mA cm^{-2} in a testing period of 100 h, as shown in Fig. 6, from 0.02 to 0.65 Ω cm^2 (32.5 times increase) and 1.38 to 1.59 Ω cm^2 (~1.2 times increase), respectively. As a result, the performance of the LSCF cathode degraded simultaneously about 3.4% for the

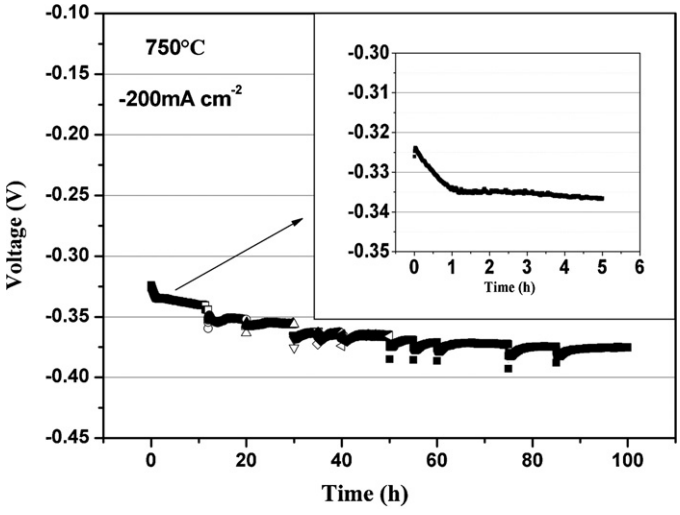

Fig. 7. Polarization curves of the half-cell with LSCF + YSZ composite cathode as a function of cathodic current passage of 200 mA cm^{-2} at 750 °C.

first 5 h of test and the overall degradation within the 100 h test was 15.6%, which is shown in Fig. 7. Both the cell and half-cell tests presented the same order of magnitude in performance degradation, suggesting that the performance degradation of the cells with impregnated LSCF cathodes is mainly caused by the composite cathode.

The performance degradation of cells with the LSCF-based cathodes has been studied previously [3,19,25,26], two possible mechanisms for the degradation have been proposed [19], that is, the instability of the LSCF, which leads to either forming resistive $SrZrO_3$ by reaction with the YSZ electrolyte or Sr releasing from the LSCF to form probably SrO at interfaces and reduce Sr content in the LSCF; and the coarsening of the microstructure of the LSCF cathodes, which increases both the ohmic and activation polarizations due to reduction in the connection between LSCF particles and the active surface area. If a new resistive phase were formed at the interfaces, the ohmic resistance would have increased significantly. However, this is not suggested by the result from the half-cell test, in which the ohmic resistance increased only to 1.2 times in contrast to an increase to 32.5 times in the polarization resistance within 100 h of test. On the other hand, all the tests were conducted at 750 °C, at which the reaction between the LSCF and the YSZ is not expected in such a short period of testing time. Therefore, microstructure coarsening of the impregnated LSCF in

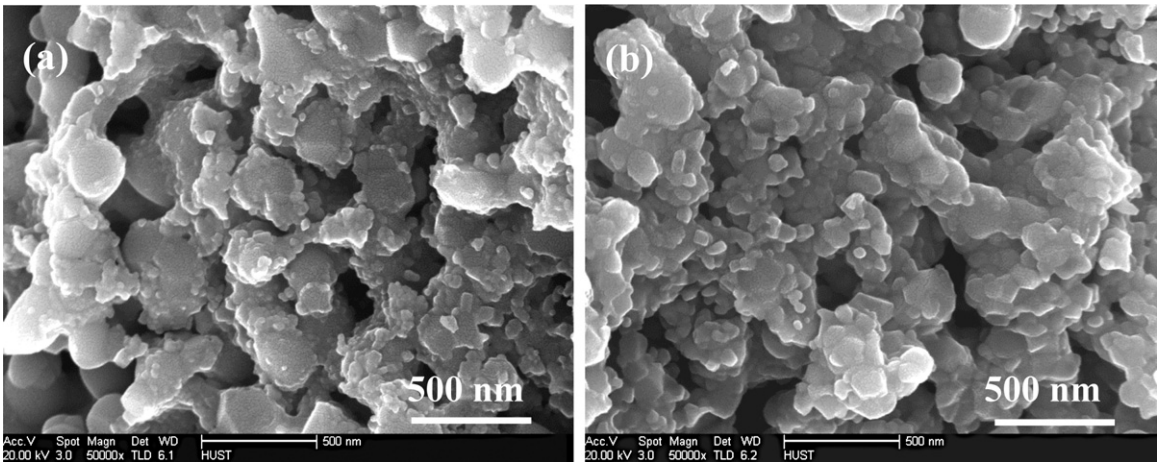

Fig. 8. SEM micrographs of the button half-cell cross-section: (a) before testing; (b) after testing.

the composite cathode is considered the reason for the performance degradation of the cells. Fig. 8 shows SEM micrographs of fractured cross-section of the half-cell before and after the test. Uniformly distributed and well connected fine LSCF particles were observed on the surface of the YSZ scaffold in the LSCF + YSZ composite cathode prior to the test (Fig. 8a), and the LSCF particles became larger after 100 h test without the presence of well connected fine LSCF particles (Fig. 8b), which supports the above expectation that the microstructure coarsening is the reason for the fast cell performance degradation and indicates the need for further development on preventing the growth of the impregnated LSCF particles during cell operation.

4. Conclusions

From the present study, the following conclusions can be made:

(1) Mixed conducting perovskite LSCF can be used in cells with large active area (9 cm × 9 cm) as the cathode, together with the YSZ electrolyte, in the absence of the GDC buffer layer by solution impregnation method at lower temperature, which circumvents issues caused by thermal coefficient mismatch and high temperature chemical incompatibility between LSCF and YSZ.
(2) The amount of the LSCF loaded in YSZ porous structure is critical for the cell performance, and a peak power density of 473 mW cm^{-2} was achieved at 750 °C with a LSCF loading of 1.3 mg cm^{-2}. Overloading the YSZ scaffold with LSCF caused significant mass transport polarization.
(3) The performance degradation of the cells with the LSCF + YSZ composite cathodes is attributed to the growth and coalescence of fine LSCF particles, a method that prevents the microstructure coarsening is desired.

Acknowledgements

This research was financially supported by the National Science Foundation of China (50571038, 60804031) and the national “863” project (2006AA05Z148). SEM examination was assisted by the Analytical and Testing Center of Huazhong University of Science and Technology.

References

[1] P. Hjalmarsson, M. Søgaard, M. Mogensen, Solid State Ionics 179 (2008) 1422–1426.
[2] Y.L. Liu, C. Jiao, Solid State Ionics 176 (2005) 435–442.
[3] S.P. Simner, M.D. Anderson, M.H. Engelhard, J.W. Stevenson, Electrochemical and Solid-State Letters 9 (2006) A478–481.
[4] W. Guo, J. Liu, Y. Zhang, Electrochimica Acta 53 (2008) 4420–4427.
[5] C. Lu, S. An, W.L. Worrell, J.M. Vohs, R.J. Gorte, Solid State Ionics 175 (2004) 47–50.
[6] J.M. Vohs, R.J. Gorte, Advanced Materials 21 (2009) 943–956.
[7] S.P. Jiang, Materials Science and Engineering: A 418 (2006) 199–210.
[8] X. Xu, Z. Jiang, X. Fan, C. Xia, Solid State Ionics 177 (2006) 2113–2117.
[9] S.P. Jiang, W. Wang, Journal of the Electrochemical Society 152 (2005) A1398–A1408.
[10] F. Liang, J. Chen, S.P. Jiang, B. Chi, J. Pu, Li Jian, Electrochemical and Solid-State Letters 11 (2008) B213–B216.
[11] Y. Liu, S. Hashimoto, K. Yasumoto, K. Takei, M. Mori, Y. Funahashi, Y. Fijishiro, A. Hirano, Y. Takeda, Current Applied Physics 9 (2009) S51–S53.
[12] M. Sahibzada, S.J. Benson, R.A. Rudkin, J.A. Kilner, Solid State Ionics 113–115 (1998) 285–290.
[13] J. Chen, F. Liang, B. Chi, J. Pu, S.P. Jiang, Li Jian, Journal of Power Sources 194 (2009) 275–280.
[14] Y. Huang, K. Ahn, J.M. Vohs, R.J. Gorte, Journal of the Electrochemical Society 151 (2004) A1592–1597.
[15] Y. Huang, J.M. Vohs, R.J. Gorte, Journal of the Electrochemical Society 151 (2004) A646–A651.
[16] Y. Huang, J.M. Vohs, R.J. Gorte, Journal of the Electrochemical Society 152 (2005) A1347–A1353.
[17] J. Chen, F. Liang, L. Liu, S. Jiang, B. Chi, J. Pu, J. Li, Journal of Power Sources 183 (2008) 586–589.
[18] A. Mai, V.A.C. Haanappel, S. Uhlenbruck, F. Tietz, D. Stöver, Solid State Ionics 176 (2005) 1341–1350.
[19] F. Tietz, A. Mai, D. Stöver, Solid State Ionics 179 (2008) 1509–1515.
[20] S.P. Jiang, Solid State Ionics 146 (2002) 1–22.
[21] L. Kindermann, D. Das, H. Nickel, K. Hilpert, Solid State Ionics 89 (1996) 215–220.
[22] H.L. Lein, K. Wiik, T. Grande, Solid State Ionics 177 (2006) 1795–1798.
[23] S.P. Jiang, Journal of Power Sources 124 (2003) 390–402.
[24] J. Larminie, A. Dicks, Fuel Cell Systems Explained, John Wiley & Sons, Ltd., 2000, pp. 298–300.
[25] A. Mai, M. Becker, W. Assenmacher, F. Tietz, D. Hathiramani, E. Ivers-Tiffée, D. Stöver, W. Mader, Solid State Ionics 177 (2006) 1965–1968.
[26] H. Yokokawa, H. Tu, B. Iwanschitz, A. Mai, Journal of Power Sources 182 (2008) 400–412.